diffusion-fundamentals

The Open-Access Journal for the Basic Principles of Diffusion Theory, Experiment and Application

How Two Pairs of Gradient Pulses Give Access to New Information about Molecular Dynamics

Paul T. Callaghan

MacDiarmid Institute for Advanced Materials and Nanotechnology
School of Chemical and Physical Sciences
Victoria University of Wellington, New Zealand

Abstract
Pulsed Gradient Nuclear Magnetic Resonance provides direct insight regarding the translational motion of spin-bearing molecules. These methods gain a second dimension when the simple gradient pulse pair is enhanced by a second pair. Where the motion encoding of the two pairs is opposite, flow effects are removed from the echo attenuation, making it possible to measure diffusion in the presence of shear flow, or to measure the stochastic part of dispersive flow, and in particular the velocity auto-correlation function. Where the gradient pulse pairs are stepped in independent dimensions, two-dimensional experiments become possible. One class (Fourier-Fourier) is the Velocity Exchange (VEXSY) experiment in which flow velocities may be correlated at different times. Another class (inverse Laplace-inverse Laplace) is the diffusion correlation (DDCOSY) or diffusion exchange (DEXSY) experiment. This approach has proven of particular value in ascertaining local anisotropies in globally isotropic systems, as well as in the model-free measurement of exchange effects.

1. Introduction

In this year of 2005 we celebrate the achievement of Albert Einstein in elucidating Brownian motion and giving us a new mathematical description for self-diffusion (1). In addition to explaining the role of thermal energy in determining diffusion, Einstein reformulated Fick's Law in statistical terms, giving us the relation

$$\frac{\partial \Psi(\mathbf{r},t)}{\partial t} = D\nabla^2\Psi(\mathbf{r},t) \qquad (1)$$

where $\Psi(\mathbf{r},t)$ is the probability of finding a particle at position **r** at time *t*. Using a propagator $P_s(\mathbf{r} \mid \mathbf{r}',t)$ to describe the probability that a particle starting at **r** would move to **r'** after time *t*, and noting $\Psi(\mathbf{r}',t) = \int \Psi(\mathbf{r},0)P_s(\mathbf{r} \mid \mathbf{r}',t)d\mathbf{r}$, Fick's law can be rewritten

$$\frac{\partial P_S}{\partial t} = D\nabla'^2 P_S \qquad (2)$$

Under the initial condition $P_s(\mathbf{r} \mid \mathbf{r}',0) = \delta(\mathbf{r}' - \mathbf{r})$, the solution to Fick's law for a freely diffusing particle, also obtained by Einstein, was

$$P_s(\mathbf{r} \mid \mathbf{r}', t) = (4\pi Dt)^{-3/2} \exp(-\frac{(\mathbf{r}' - \mathbf{r})^2}{4Dt}) \quad (3)$$

The science of self-diffusion measurement gained an enormous boost with the discovery of the NMR spin echo by Erwin Hahn (2). Hahn had sufficient insight to realise that this spin echo amplitude would be affected my molecular self-diffusion, a fact that was brought to realisation through the work of E.O. Stejskal and J.E. Tanner (3).

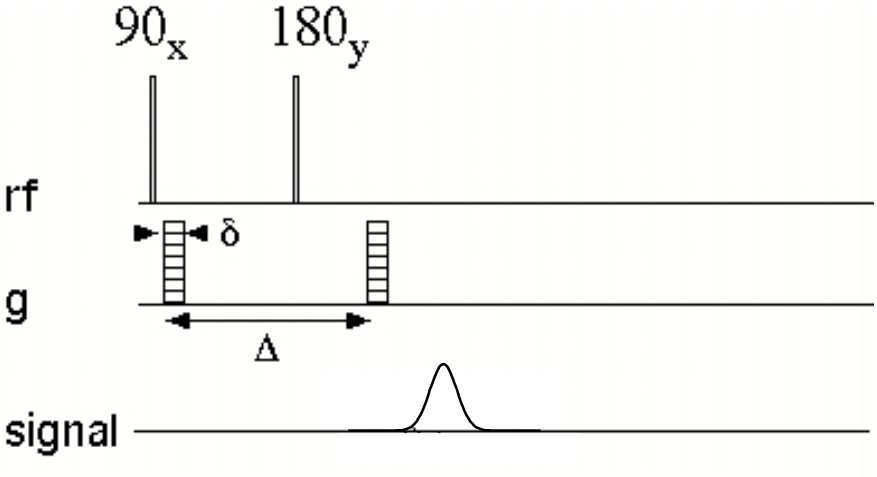

Figure 1: Basic Pulsed Gradient Spin Echo sequence

Each magnetic field gradient pulse imparts to the nuclear spins a precessional phase that depends on the spatial location of the molecule which contains that spin (typically a proton in the hydrogen of some molecule). Magnetic field gradients are produced by adding to the NMR polarising field, $\mathbf{B}_0$, an additional inhomogeneous field, **B**. where typically, $|\mathbf{B}| << |\mathbf{B_0}|$. Consider the gradient in the component of **B** along $\mathbf{B}_0$, namely $\mathbf{g} = \nabla B_z$, where the direction of $\mathbf{B}_0$ defines the laboratory *z*-axis. The Larmor precession of the spin in the presence of that gradient is a sum of two terms, one arising from the polarising field and one from the gradient, *viz*, $\omega = \gamma B_0 + \gamma \mathbf{g}.\mathbf{r}$, where **r** is the position of the spin-bearing molecule. If this gradient is applied as a pulse for a duration δ, then, relative to the average precession, that spin at position **r**, will have acquired an additional phase $\gamma \mathbf{g}.\mathbf{r}\delta$. In the spin echo experiment the phase shifts from each gradient pulse will be of opposite sign, because of the 180° rf pulse inserted between

the pulses. In NMR we represent phase shifts via complex exponential factors, $\exp(i\gamma \mathbf{g}.\mathbf{r}\delta)$.

Interestingly, Stejskal and Tanner chose to use the propagator language of Einstein's formulation, in laying out the theoretical basis of the Pulsed Gradient Spin Echo (PGSE) NMR method, so that for rectangular gradient pulses of duration δ and amplitude **g** separated by a time Δ, (see figure 1) the normalised echo amplitude (*ie* $E(g) = A(g)/A(0)$), may be written

$$E(g) = \iint P(\mathbf{r})\exp(-i\gamma\delta\mathbf{g}.\mathbf{r})P(\mathbf{r} \mid \mathbf{r}', \Delta)\exp(i\gamma\delta\mathbf{g}.\mathbf{r}')d\mathbf{r}d\mathbf{r}' \qquad (4)$$

Later Kärger and Heink (4) introduced the idea of an average propagator

$$\overline{P}(\mathbf{R}, \Delta) == \int P(\mathbf{r})P(\mathbf{r} \mid \mathbf{r} + \mathbf{R}, \Delta)d\mathbf{r} \qquad (5)$$

so that the normalised Echo amplitude could be more simply written

$$E(\mathbf{g}) = \int \overline{P}(\mathbf{R}, \Delta)\exp(i\gamma\delta\mathbf{g}.\mathbf{R})d\mathbf{R} \qquad (6)$$

From the gaussian nature of $\overline{P}(\mathbf{R}, \Delta)$ in the case of simple unrestricted self-diffusion, the normalised Echo amplitude follows as $E(\mathbf{g}) = \exp(-\gamma^2\delta^2 g^2 D\Delta)$. A more exact treatment (for example using the Bloch-Torrey equation (5)) shows that Delta has to be replaced by the reduced time $\Delta - \delta/3$ (the Stejskal-Tanner relation). Note that in the case where molecules also flow with velocity **v**, the echo amplitude contains both an attenuation term and a phase shift term, *viz*, $E(\mathbf{g}) = \exp(-\gamma^2\delta^2 g^2 D\Delta + i\gamma\delta\mathbf{g}.\mathbf{v}\Delta)$. This means that the PGSE NMR experiment can also be used to measure flow.

For several decades PGSE NMR has served as a valuable tool in obtaining molecular self-diffusion coefficients for a wide class of molecules in the liquid state (6-11), with the great advantage of NMR that spectral resolution has enabled molecular specificity in the measurement. In its application to the study of polymer dynamics, PGSE NMR has even enabled the observation of internal diffusional modes, revealing reptational scaling laws at length scales as small as 20 nm (12).

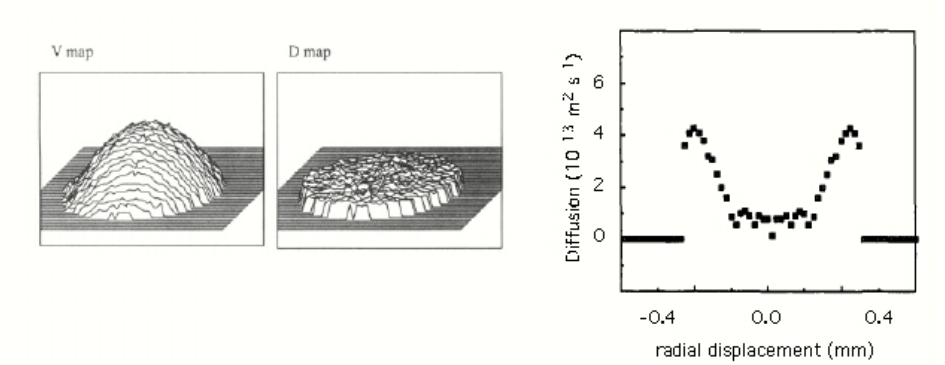

Figure 2: Images of velocity and diffusion of water molecules for a semi-dilute solution of high molecular weight PEO (0.5% w/v in water). The profile shows the enhancement of polymer diffusion in the region of high shear near the walls (adapted from reference 13).

In the 1980s, PGSE NMR was adapted to NMR imaging experiments to enable spatially localised diffusion to be studied. Figure 2 shows images of the flow velocity and the solvent water molecule self-diffusion, in the case of a semi-dilute (entangled) polymer solution passing through an 0.7 mm diameter pipe (13). Also shown is a profile across the tube in which the polymer self-diffusion is plotted. The enhancement of diffusion near the walls is indicative of entanglement tube deformation and enhanced reptational displacements (13).

Following on from the imaging perspective, it was realised that the echo attenuation in the PGSE NMR experiment, could contain a signature for non-Brownian motion, for example restricted diffusion of heterogeneous flow, and the use of a wave-vector formalism (**q**-space) (7) to describe the echo attenuation physics, greatly facilitated that approach. Here the wavevector **q** is related to the area under the gradient pulses by (7)

$$\mathbf{q} = \frac{1}{2\pi}\gamma\delta\mathbf{g} \qquad (7)$$

The Fourier relation, equation 6, can clearly be written (replacing the integral of the average propagator as an ensemble average <…>) as simply

$$E(\mathbf{q}) = \int \overline{P}(\mathbf{R},\Delta)\exp(i2\pi\mathbf{q}.\mathbf{R})d\mathbf{R} = <\exp(i2\pi\mathbf{q}.\mathbf{R})> \qquad (8)$$

The subject of wave-vector dependence of echo attenuation in single pulse pair PGSE NMR, including diffusive diffraction effects, is covered in detail elsewhere (7,14). *This article will focus on the use of different forms of gradient phase encoding.* The single gradient pulse pair approach of figure 1, while offering a wide range of applications, is not the only mode of NMR measurement of molecular translational motion. Indeed, as

we shall show here, there are phenomena where higher order gradient pulse trains are called for.

2. Self-diffusion, dispersion and velocity fluctuations

One of the most important findings of Einstein's 1905 paper on diffusion is that the (three-dimensional) molecular mean-squared displacement, σ^2 depends linearly on time, τ, as $\sigma^2(\tau) = 6D\tau$. The same Einsteinian perspective can be applied in considering other forms of molecular dispersion than that driven by thermal energy alone. Generally, dispersion is the process whereby molecules that start together in the same vicinity become separated as a result of translational motions. In thermal equilibrium, and in the absence of fluid flow, Brownian motion alone will be sufficient to induce molecular separation, although, in a porous medium, the presence of fluid/matrix interfaces may impede this motion to the extent that apparent diffusion rates will depend on the length and time scales used in making the measurement.

Once flow occurs in a porous medium, a number of other mechanisms for separating initially adjacent molecules take over and the rate of dispersion rises significantly above the diffusion "baseline". Nonetheless the ideas that underpin the theory of Brownian motion help to provide us with a mathematical language to describe flow-induced dispersion. Like diffusion, dispersion involves stochastic processes that necessitate the language of statistical physics.

Remarkably, it is possible to show that the diffusion process may be related to the molecular (Lagrangian) **velocities,** $\mathbf{u}(t)$, through the relation (15)

$$\frac{1}{2}\frac{\partial\sigma^2(\tau)}{\partial\tau} = sym\int_0^\tau <\mathbf{u}(t)\mathbf{u}(0)>dt \tag{9}$$

where $<\mathbf{u}(t)\mathbf{u}(0)>$ is the velocity autocorrelation function, strictly a tensor quantity. The symmetry operator is $sym(\mathbf{A}) = \frac{1}{2}(\mathbf{A} + \mathbf{A}^T)$. Note that the best analogy with diffusion obtains if **u** is the **stochastic velocity**, *ie*, the variation about the mean. In other words, if the total velocity is **v**, then **v**=**u**+<**v**> where for a stationary ensemble, the ensemble and time average velocities are equal. In the asymptotic case, $\tau \to \infty$, we obtain the definition of the diffusion tensor (15,16)

$$\underline{\underline{\mathbf{D}}}^* = \lim_{\tau\to\infty} sym\int_0^\tau <\mathbf{u}(t)\mathbf{u}(0)>dt \tag{10}$$

Note that we may define a frequency dependent dispersion tensor (17),

$$\underline{\underline{\mathbf{D}}}^{*}(\omega) = sym\int_0^{\infty} < \mathbf{u}(t)\mathbf{u}(0) > \exp(i\omega t)dt \tag{11}$$

where the asymptotic dispersion tensor referred to above is the zero frequency component of $\underline{\underline{\mathbf{D}}}^{*}(\omega)$.

The Pulsed Gradient Spin Echo experiment can be used to measure not only Brownian self-diffusion, but also the dispersion behaviour of fluids (18-21). Indeed the method is ideally suited to this role because it returns the true Lagrangian velocity. We may write the echo attenuation for the pulse sequence shown in figure 1, by using the spin velocities, *ie*

$$E(\mathbf{q}) = < \exp(i2\pi\mathbf{q}.\int_0^{\Delta} \mathbf{v}(t)dt > \tag{12}$$

To second order in **q** we may write

$$E(\mathbf{q}) \approx \exp(i\alpha)\exp(-\beta) \tag{13}$$

where the phase exponent $\alpha = 2\pi\mathbf{q}.\int_0^{\Delta} < \mathbf{v}(t) > dt$, arises from the mean flow

while the attenuation exponent is

$$\begin{aligned} \beta &= 2\pi^2 q^2 \left[< \left(\int_0^{\Delta} \mathbf{v}(t)dt \right)^2 > - \left(\int_0^{\Delta} < \mathbf{v}(t) > dt \right)^2 \right] \\ &= 2\pi^2 q^2 < \left(\int_0^{\Delta} \mathbf{u}(t)dt \right)^2 > \end{aligned} \tag{14}$$

One intriguing aspect of dispersion concerns the degree to which molecular separations are inherently reversible or irreversible. For example, in pipe flow, the Poiseuille distribution has the effect of separating molecules on adjacent streamlines, in other words inducing a distribution of phases $2\pi\mathbf{q}.\int_0^{\Delta} < \mathbf{u}(t) > dt$ and an echo attenuation via the first term in equation 14. However, provided the molecules remain on those streamlines, a flow reversal will return them to adjacency. Should they diffuse across stream lines, however (22), then irreversibility sets in, as revealed through the fluctuations apparent in

the correlation term $< \left(\int_0^{\Delta} \mathbf{u}(t)dt \right)^2 >$. We shall see that the way to discriminate between the reversible and irreversible dispersive contributions is through the use of higher order gradient pulse trains.

3. Double pulse pairs and multiple pulse trains

In 1954 Carr and Purcell (23) showed that a repetitive train of 180° rf pulses applied during a period of free precession, could sustain the echo envelope for an especially long time. Further, they noted that when the spin bearing molecules were in flow, the echo train was perturbed, there being a quite different perturbation on odd and even echoes in the pulse train. Consider the double PGSE pulse pair shown in figure 3.

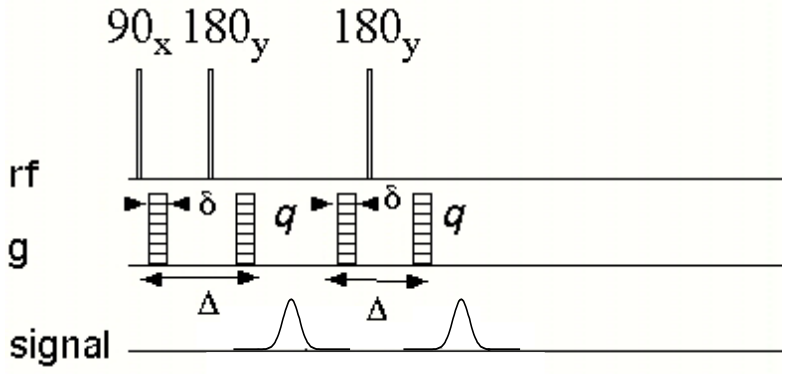

Figure 3: Double PGSE NMR sequence in which pairs of gradient pulses of opposite sense encode are applied in succession.

In this sequence the phase factors which arise for each gradient pulsed are successively positive, negative, negative and positive. Thus the net effect is that each successive pair encodes for motion in an opposite sense (7,14). Again, using velocities to describe the spin displacements, we may write for the echo attenuation (24,25)

$$E_D(\mathbf{q}) = < \exp(i2\pi\mathbf{q}.\int_0^{\Delta} \mathbf{u}(t)dt - i2\pi\mathbf{q}.\int_{\tau_m}^{\tau_m+\Delta} \mathbf{u}(t')dt') > \qquad (15)$$

Note that the subtraction of the two phase terms means that only **fluctuations** in **v**(t) are apparent and all mean flow terms are cancelled. This approach has been used to measure diffusion of macromolecules in the presence of heterogeneous (pipe) flow. For small molecules, streamline-crossing effects (Taylor dispersion) becomes important. Codd *et al* (26) applied the double PGSE NMR method to measure the irreversible component of Taylor dispersion for molecules in pipe flow, as shown in figure 4, comparing with the much higher apparent dispersion when a single PGSE pulse pair is applied.

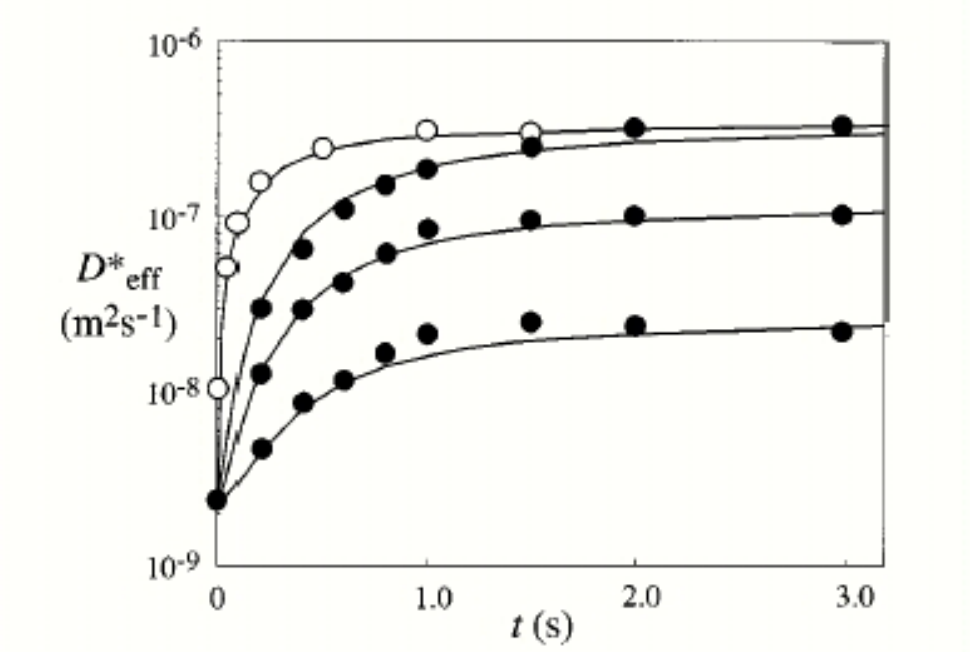

Figure 4: Dispersion coefficients obtained for different encoding times for octane flowing in a 150 micron diameter pipe. The open circles show the effective total dispersion as measured from the initial attenuation of a single PGSE experiment for octane flowing with U = 2.6 mm s^{-1}. The solid circles show the stochastic dispersion results obtained using the double PGSE variant, the three values of U being 2.6 mm s^{-1}, 1.6 mm s^{-1} and 0.7 mm s^{-1}. Superposed on the experimental data are the theoretical curves generated using a propagator eigenmode expansion approach (adapted from reference 26).

In the low **q** limit, equation 15 may be used to yield an apparent dispersion coefficient (25)

$$D^* = \frac{1}{4\Delta}\left[\int_0^{\Delta}\int_0^{\Delta} < u(t)u(t') > dtdt' - 2\int_0^{\Delta}\int_{\tau_m}^{\tau_m+\Delta} < u(t)u(t') > dtdt' + \int_{\tau_m}^{\tau_m+\Delta}\int_{\tau_m}^{\tau_m+\Delta} < u(t)u(t') > dtdt'\right]$$

$$= \frac{1}{2\Delta}\int_0^{\Delta}\int_0^{\Delta} < u(t)u(t') > dtdt' - \frac{1}{2\Delta}\int_0^{\Delta}\int_{\tau_m}^{\tau_m+\Delta} < u(t)u(t') > dtdt' \qquad (16)$$

Provided the encoding time Δ is much shorter than the correlation time for fluctuations in the velocity, one obtains (14,25)

$$< u^2 > - < u(\tau_m)u(0) >= \frac{2D^*}{\Delta} \qquad (17)$$

In other words, the double PGSE NMR method may be used to directly measure the velocity autocorrelation function (VACF) in stochastic flow, for example for fluid flow through porous media. Figure 5 shows VACF data obtained for flow though latex bead packs using this approach (25).

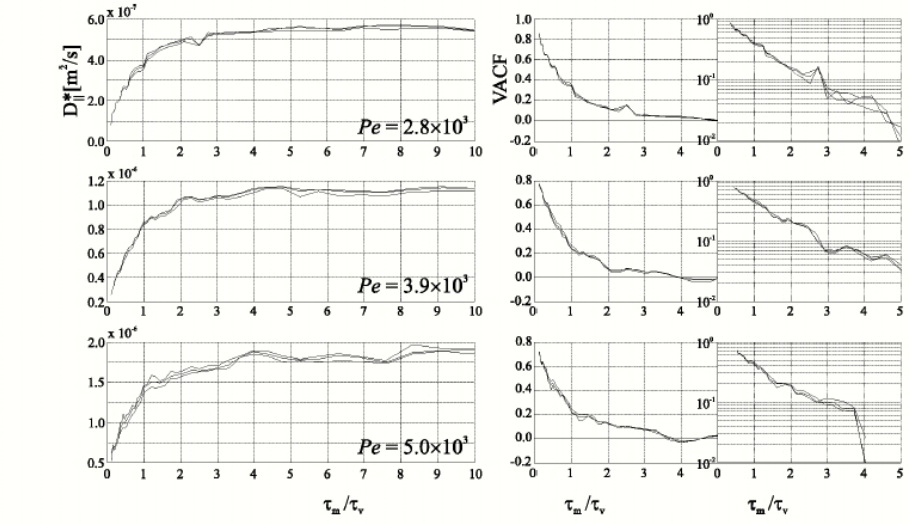

Figure 5: Effective dispersion coefficients and VACF plots, obtained for flow of water in a bead pack of bead diameter 500 microns (adapted from reference 25).

More generally, multiple pairs of gradient pulses may be applied in succession to provide a frequency domain analysis of fluctuations in dispersion, as shown in figure 6 (27). The theory behind such experiments is described elsewhere (14,27,28).

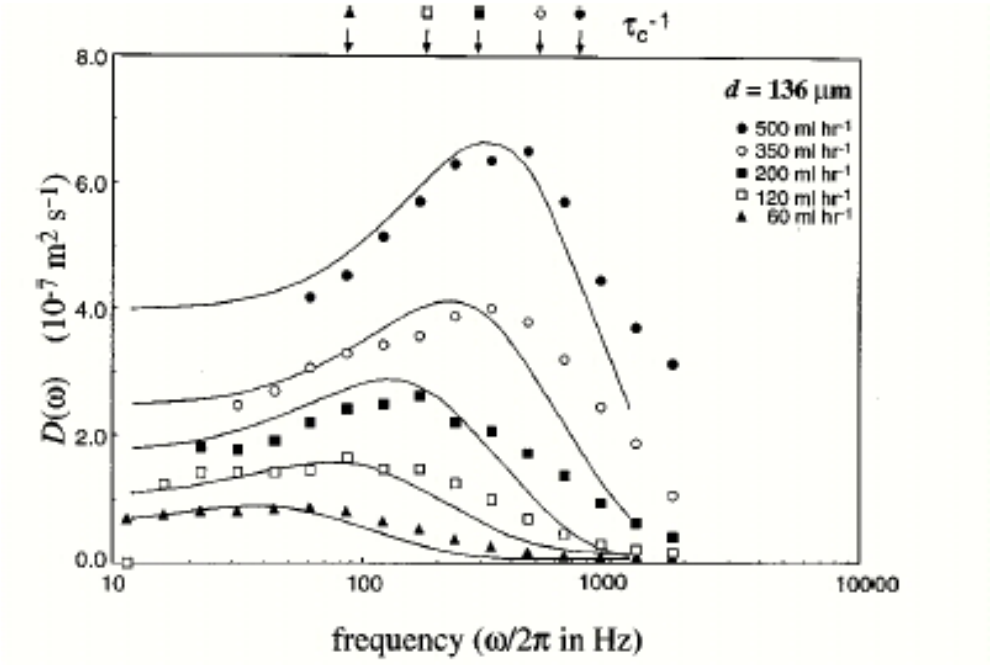

Figure 6: The effective transverse dispersion coefficients, $D(\omega)$, measured at each frequency $f = 1/T$ over the range of flow rates as shown, for a 136 μm diameter bead pack (adapted from reference 27).

4. Velocity Exchange Spectroscopy (VEXSY)

Of course if two pairs of gradient pulses are applied, it is possible to vary the **q** vectors of each independently (29). Such an approach is of particular interest in the case of fluctuating flows. Now the signal may be written in terms of two wavevectors, $\mathbf{q}_1$ and $\mathbf{q}_2$ as

$$E(\mathbf{q}_1,\mathbf{q}_2) = \iint \overline{P}_2(\mathbf{R}_1,\Delta;\mathbf{R}_2,\Delta;\tau_m)\,\exp(\mathrm{i}\,2\pi\,\mathbf{q}_1\cdot\mathbf{R}_1)\,\exp(\mathrm{i}\,2\pi\,\mathbf{q}_2\cdot\mathbf{R}_2)\,\mathrm{d}\mathbf{R}_1\,\mathrm{d}\mathbf{R}_2 \tag{18}$$

If $\mathbf{q}_1$ and $\mathbf{q}_2$ are varied independently of each other, the echo attenuation function is now two dimensional in $\mathbf{q}_1$ and $\mathbf{q}_2$. Inverse Fourier transformation with respect to the two independent **q** spaces yields a two-dimensional distribution function $\overline{P}_2(\mathbf{R}_1,\Delta;\mathbf{R}_2,\Delta;\tau_m)$. This function represents the two-time probability density of finding displacements $\mathbf{R}_1$ in the first and $\mathbf{R}_2$ in the second encoding interval of duration Δ, separated by a mixing time τ_m. $\overline{P}_2(\mathbf{R}_1,\Delta;\mathbf{R}_2,\Delta;\tau_m)$ can be decomposed as (29)

$$\overline{P}_2(\mathbf{R}_1,\Delta;\mathbf{R}_2,\Delta;\tau_m) = \overline{P}_1(\mathbf{R}_1,\Delta)\,\mathcal{P}_V(\mathbf{R}_1,\Delta\,|\,\mathbf{R}_2,\Delta;\tau_m) \tag{19}$$

where $\overline{P}_1(\mathbf{R}_1,\Delta)$ is the propagator during the first interval (identical to the propagator in the second interval under steady state flow), and $\mathcal{P}_V(\mathbf{R}_1,\Delta\,|\,\mathbf{R}_2,\Delta;\tau_m)$ is the conditional probability that, if a displacement by $\mathbf{R}_1$ occurs during the first interval Δ, then a displacement $\mathbf{R}_2$ will occur during the second time interval of equal duration to the first, delayed by a mixing time τ_m.

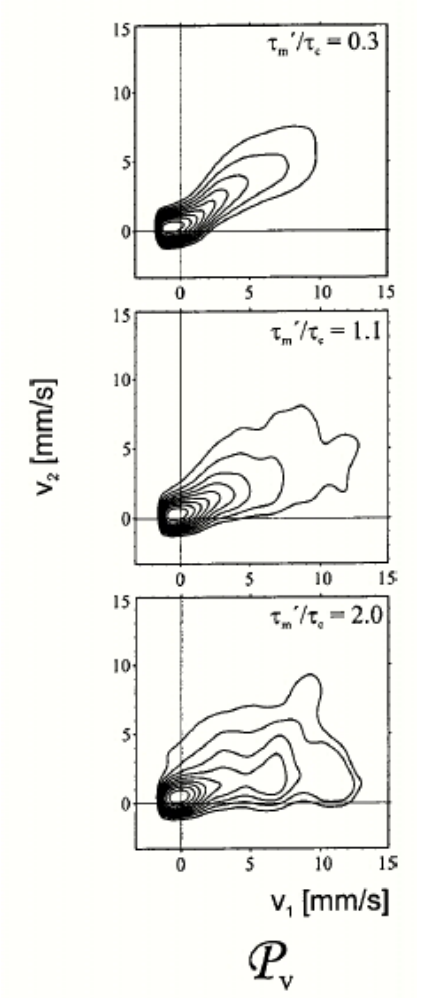

Note that $\mathcal{P}_V$ describes the conditional probability between *displacements* in the VEXSY case, as compared to $P(\mathbf{r}\,|\,\mathbf{r}',t)$ that relates *positions* at times separated by *t*.

Figure 7 shows an example of a measurement of $\mathcal{P}_V(\mathbf{R}_1,\Delta\,|\,\mathbf{R}_2,\Delta;\tau_m)$ for flow of water in a bead pack for a Peclet number (<v>*l*/*D* where *l* is the pore size and *D* the molecular self-diffusion coefficient) of $9\text{x}10^3$. The characteristic patterns are of particular interest in elucidating flow correlations. In the upper frame, where the mixing time is shorter than the fluctuation correlation time, strong velocity correlations are apparent.

Figure 7: Conditional probabilities obtained from VEXSY experiments for water flow in a bead pack, with a Peclet number of $9\text{x}10^3$ (adapted from reference 30)

The shape of $\mathcal{P}_V\left(Z_1,\Delta\,|\,Z_2,\Delta;\tau_m'\right)$ can be separated into three regions (30). For small velocities, the contour lines lie horizontally, i.e. the conditional probability of finding a particular velocity after the mixing time is independent of the value before the mixing time. This accounts for spins which reside in quasi-static pools or which flow slowly so that their displacements are essentially dominated by the contributions of random self-diffusion. For intermediate velocities, a strong correlation is found. This subset of spins follows streamlines but have not yet encountered geometrical obstacles which can lead to mechanical dispersion and therefore to a change of velocities. The fastest particles

however, have travelled distances comparable to the structural size of the system, in this case, the bead size, and have changed their direction and/or magnitude of velocity.

5. Diffusion Diffusion Exchange (DEXSY)

In the VEXSY experiment, the inverse two-dimensional Fourier transformation revealed the propagator associated with velocity fluctuations. In systems that are purely diffusive, such Fourier inversion is not necessarily the best means of revealing exchange effects. In particular, consider a system in which there exists exchange of molecules between one compartment and another, these compartments having different local values of the self-diffusion coefficient. In that case one might expect that the diffusion coefficient of any one molecule may change as the molecule exchanges between compartments. One very effective means of revealing this phenomenon is via a two-dimensional experiment in which two pairs of gradient pulses, separated by a mixing time, are used to independently encode for diffusion. In essence the pulse sequence is identical as for the VEXSY experiment, but the data analysis is very different.

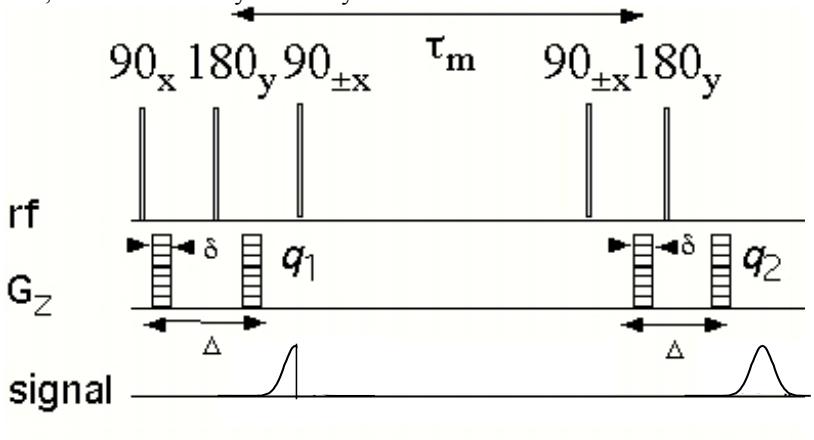

Figure 8: Pulse sequence used for DEXSY and VEXSY. In the case of VEXSY, where inverse Fourier transformation is to be used, bipolar gradients are preferable.

With purely diffusive motion, the echo attenuation function consists of an exponential decay, multi-exponential if more than two diffusion modes are present. If instead of Fourier inversion one uses Laplace inversion (31,32), the distribution of diffusion coefficients is revealed. Where 2-dimensional inverse Laplace transformation is used (33), one may obtain a map in which the two diffusion behaviours at the separated times are directly compared (34,35). This experiment is known as diffusion-diffusion exchange, or DEXSY.

The process of 2-D inverse Laplace analysis is not straightforward but major advances have been made in the last two years (33) that enable the process to be carried out robustly. For an application of the method (36) see figure 9. Here a hollow polymer

particle with porous walls permits exchange of dextran between the particle interior (where the dextran diffusion is limited by restriction to that of the containment sphere), to the exterior water solvent, where the diffusion is free.

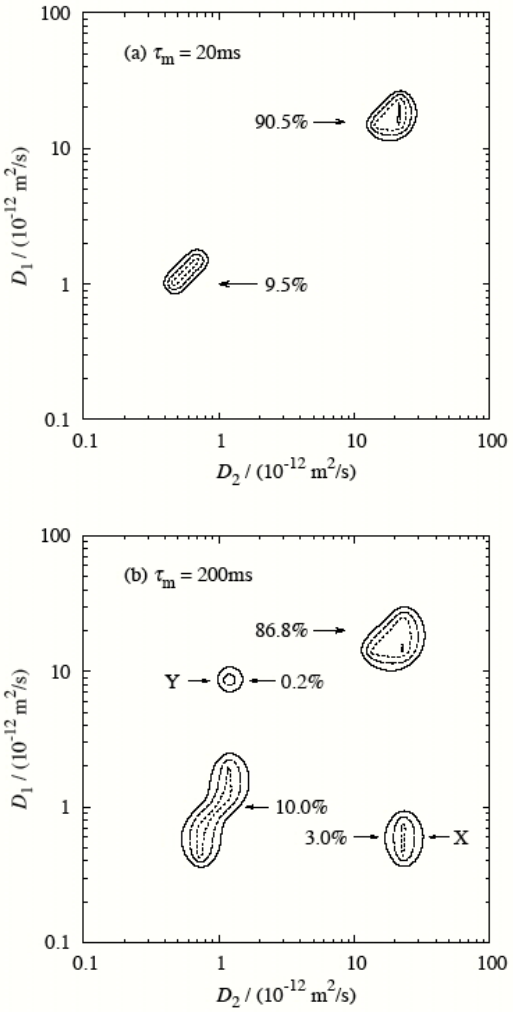

Figure 9: DEXSY experiment at two different mixing times for dextran diffusion between the interior and exterior of a porous polymer capsule (adapted from reference 36).

At short exchange times, two peaks are seen on the diagonal, corresponding to the free and sphere-bound dextran respectively. At longer exchange times off-diagonal peaks appear arising from dextran that have exchanged locations. Measurement of the intensity of these off-diagonal peaks permits a model-free analysis of the exchange process.

6. Diffusion-Diffusion Correlation (DDCOSY)

A quite different diffusion-diffusion analysis based on 2D Laplace inversion, is diffusion-diffusion correlation (DDCOSY) (34,35). The DDCOSY experiment has particular utility for the investigation of local diffusion anisotropy in a sample that is macroscopically isotropic. Examples include poly-domain lyotropic liquid crystals, porous solids, polymer melts or semi-dilute solutions and strained elastomers. In the first example the water solvent may be trapped in thin (ie ~100 Å) sheets between lamellar bilayers with the diffusion severely restricted normal to the bilayer and relatively free within the sheet. We refer to such a system as locally 2-dimensional and note that the crossover length scale is the domain size, which may be greater than or on the order of many tens of microns. In the second case the porous medium may comprise a network of channels so that absorbed fluid is restricted to diffuse in one dimension along the channel axis. This locally 1-dimensional system will exhibit a crossover to isotropy on a length scale corresponding to the representative volume, *ie*, the inter-pore spacing. Figure 10 shows the relevant local geometry in which the polar axis is used to define the direction of the applied gradient.

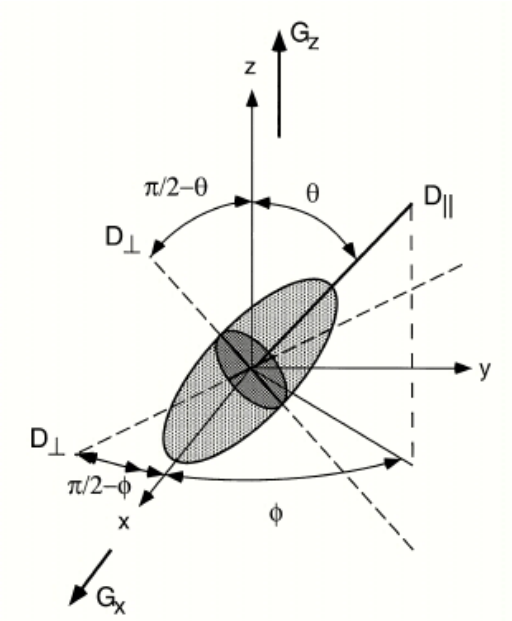

Figure 10: Schematic of local diffusion anisotropy.

Under locally anisotropic motion the spins have diffusion coefficient $D_{||}$ along a particular director at polar angle θ and azimuth ϕ, and $D_{\perp}$ in the plane normal to this director. For convenience we can choose two representative orthogonal axes in the plane of $D_{\perp}$ with (polar, azimuth) directors, (π/2− θ , ϕ) and (π /2, π/2− ϕ) as shown.

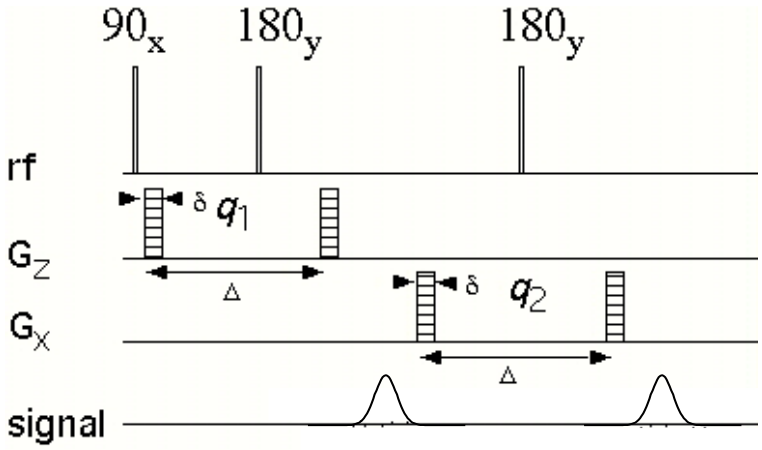

Figure 11: DDCOSY pulse sequence. In this experiment the two pairs of gradient pulses are applied in close time proximity with the aim of correlating motion along different axes.

The DDCOSY double Pulsed Gradient echo experiment is shown in figure 11. Here the spin magnetisation is recycled through two successive gradient encoding pairs, G_1 and G_2 whose q-vectors are defined respectively by $\mathbf{q}_1$ and $\mathbf{q}_2$, and may be applied in different directions, so that we can correlate the (D_1,D_2) distribution when the successive directions are respectively collinear or orthogonal (34,35). While the spread of diffusion coefficients in the (D_1,D_2) plane will reflect the isotropic distribution of directors, it is clear that despite overall isotropy, the diffusion correlations will fundamentally differ under local anisotropy. The problem shown in figure 10 has an analytic solution for the echo attenuation,

$$E(G_{1z},G_{2z}) = \int_0^1 d\cos\theta \exp(-({q_{1z}}^2 + {q_{2z}}^2)\Delta_r[D_{||}\cos^2\theta + D_{\perp}\sin^2\theta])$$

$$E(G_{1z},G_{2x}) = \int_0^1 d\cos\theta \exp(-{q_{1z}}^2\Delta_r[D_{||}\cos^2\theta + D_{\perp}\sin^2\theta])$$

$$\text{x } (2\pi)^{-1}\int_0^{2\pi} d\phi \exp(-{q_{2x}}^2\Delta_r[D_{||}\sin^2\theta\cos^2\phi + D_{\perp}\sin^2\phi + D_{\perp}\cos^2\theta\cos^2\phi]) \quad (20)$$

These equations predict characteristic patterns for different local anisotropies.

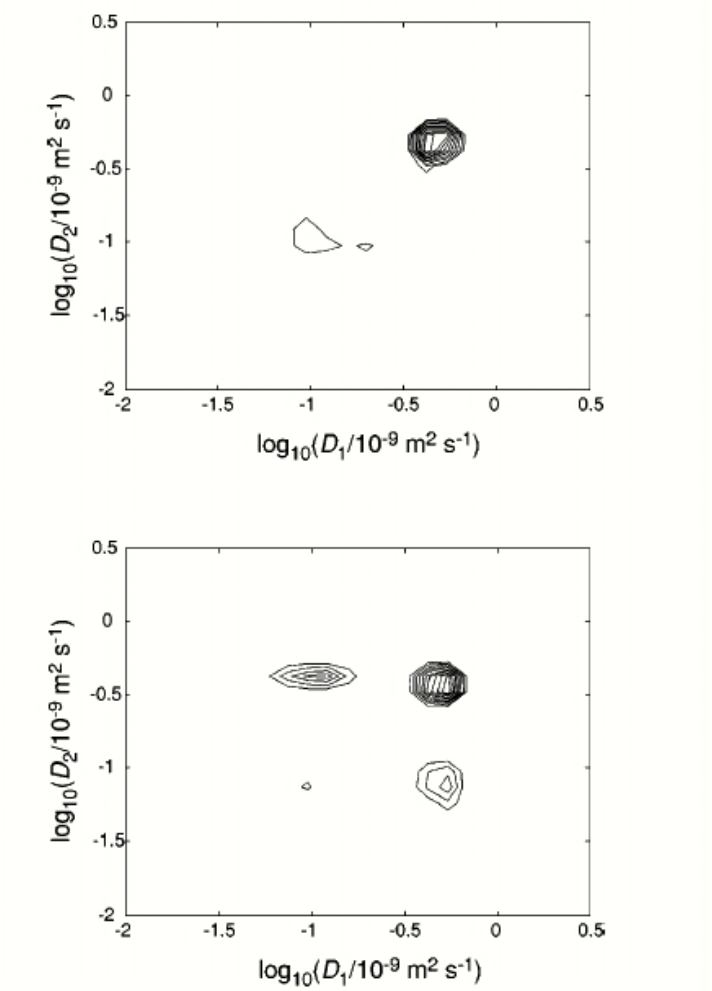

Figure 12: Diffusion-diffusion patterns in 40% C10E3/water are shown for the $E(G_{1z},G_{2z})$ experiment (which yields diagonal spectra) and the experiment $E(G_{1z},G_{2x})$ for which a distinct off-diagonal pattern is seen. It is apparent that $D_\perp = 0.1D_\parallel$ and $D_\parallel = 0.1D_\perp$ respectively (adapted from reference 35),

A test of the DDCOSY method is shown in figure 12, using the pulse sequence of figure 8 on a 40% w/w sample of the polydomain lamellar phase of the lyotropic liquid crystal, C10E3 in water. A DEXSY experiment carried out on the same system using collinear gradient pulses dramatically reveals the migration of water molecules between the local domains. These experiments indicate the potential of the DDCOSY and DEXSY

experiments to elucidate diffusion anisotropy and diffusion fluctuations in porous media and soft matter.

7. Conclusion

This review sets out to show how double PGSE NMR methods may be used to observe correlations and fluctuations for both stochastic flow (dispersion) and for diffusion within and between compartments or domains in anisotropic soft matter of porous media. Of course, the 2-dimensional approach is experimentally time consuming, with data acquisition being on the order of hours. The Inverse Laplace analysis must be treated with due care and considerable caution. Finally, the importance of long relaxation times in the case of exchange experiments is obvious.

Of course, such 2-D methods are not restricted to diffusion alone. Indeed there are a number of experiments performed where both diffusion and the flow propagator have been correlated with T_2 relaxation (33,37). Such multidimensional approaches have obvious utility. VEXSY, DEXSY and DDCOSY all allow full spectroscopic analysis in the readout (signal-acquisition) domain, thus lending themselves to heterogeneous systems or molecular mixtures

Finally, it is noted that the new science of Rheo-NMR requires that molecular properties be measured in the presence of heterogeneous flow fields. If diffusion is to be measured, the flow compensation is essential. The double PGSE method and the multi echo frequency domain PGSE method have a significant role to play in such developments.

References

1. A Einstein, *Ann. Phys.* **17**, 549 (1905)
2. E.1 L. Hahn, *Phys. Rev.,* **80**, 580 (1950)
3. E. O. Stejskal and J. E. Tanner, *J. Chem. Phys.,* **42**, 288 (1965)
4. J. Karger and W. Heink, *J. Magn. Reson*. **51**, 1 (1983).
5. H.C. Torrey, Phys. Rev. **104**, 563 (1956).
6. P.T. Callaghan, *Australian Journal of Physics* **37**, 359 (1984).
7. P.T. Callaghan, *"Principles of NMR Microscopy"*, 492 pp, Oxford University Press, (1991)
8. W. S.Price, *Concepts in magnetic resonance*, **9**, 299 (1997); **10**, 197 (1998)
9. P. Stilbs, Progr. *Nucl. Magn. Reson. Spectroscopy*, **19**, 1 (1987).
10. J. Karger, H. Pfeifer and W. Heink, *Advances in Magn. Reson*. **12**, 1, (1988).
11. R.J. Hayward, K.J. Packer and D.J. Tomlinson, *Mol. Phys.* **23**, 1083
12. M. E. Komlosh and P. T. Callaghan, *J. Chem Phys* **109**, 10053 (1998)
13. Y. Xia and P.T. Callaghan, "*Macromolecules*, **24**, 4777-4786 (1991)
14. P.T. Callaghan, S.L. Codd and J.D. Seymour, *Concepts in Magnetic Resonance*, **11**, 181-202 (1999).
15. D. L. Koch, and J. F. Brady, *AIChE J., 180*, 387 (1987).
16. J. F. Brady in *Hydrodynamics of Dispersed Media*, J. P. Hulin, A. M. Cazabat, E. Guyon and F. Carmona, eds., Elsevier, New York (1990).
17. J. Stepisnik, *Physica B*, **104B**, 350 (1981).

18. J. D. Seymour, and P. T. Callaghan, *AIChE J.,* **43**, 2096 (1997)
19. U. Tallarek, D. van Dusschoten, H. Van As, E. Bayer and G. Guiochon, *J. Phys. Chem. B*, **102**, 3486 (1998)
20. B. Manz, P. Alexander and L.F.Gladden, *Phys. Fluids*, **11**, 259 (1999)
21. J.J. Tessier, K.J. Packer, J-F. Thovert and P.M. Adl;er, *AIChEJ*, **43**, 1653 (1997)
22. C. Van Den Broeck, *Physica A*, **168**, 677 (1990).
23. H.Y. Carr and E.M. Purcell, *Phys. Rev*. **94**, 630 (1954).
24. A. A. Khrapitchev and P. T. Callaghan, *Journal of Magnetic Resonance* **152**, 259 (2001) .
25. A. A. Khrapitchev and P. T. Callaghan, *Phys. Fluids* **15**, 2649 (2003)
26. S.L.Codd, B.Manz, J.D. Seymour and P.T. Callaghan, *Physical Review E* , **60** R3491 (1999)
27. P.T. Callaghan and S.L. Codd, *Physics of Fluids*, **13** , 421 (2001).
28. P.T. Callaghan and J. Stepisnik, *Advances in Magnetic and Optical Resonanc*e, **19**, 325 (1996)
29. P.T. Callaghan and B. Manz, *Journal of Magnetic Resonance*, **A106**, 260 (1994)
30. A. A. Khrapitchev, S. Stapf and P. T. Callaghan, *Phys Rev E* **66**, 051203-1 (2002)
31. Lawson C.L. and R.J.Hanson, *Solving least squares problems*, Prentice-Hall, Englewood Cliffs, N.J (1974).
32. S.W. Provencher, *Comput. Phys. Commun.* **27** 229 (1982).
33. Y.Q. Song, L. Venkataramanan, and M.D. Hürlimann, *J. Magn. Reson.* **154**, 261 (2002).
34. P.T. Callaghan, S. Godefroy and B.N. Ryland , *Magnetic Resonance Imaging* **21**, 243 (2003)
35. P.T. Callaghan and I Fúro, *Journal of Chemical Physics*, **120**, 4032 (2004)
36. Y. Qiao, P. Galvosas, T. Adalsteinsson, M. Schönhoff and P. T. Callaghan' *J. Chem. Phys* (in press)
37. S. Godefroy, L.K. Creamer, P.J. Watkinson and P.T. Callaghan, in *Magnetic Resonance in Food Science: latest developments* eds P.S. Belton, G.A.Webb, A.M.Gil and ID. Rutledge, (Royal Society of Chemistry, Cambridge, 2003)